RESEARCH ARTICLE

Extrusion-Based Bioprinting through Glucose-Mediated Enzymatic Hydrogelation

Enkhtuul Gantumur, Masaki Nakahata, Masaru Kojima and Shinji Sakai*

Department of Materials Engineering Science, Graduate School of Engineering Science, Osaka University, Toyonaka, Osaka 560-8531, Japan

Abstract: We report an extrusion-based bioprinting approach, in which stabilization of extruded bioink is achieved through horseradish peroxidase (HRP)-catalyzed cross-linking consuming hydrogen peroxide (H_2O_2) supplied from HRP and glucose. The bioinks containing living cells, HRP, glucose, alginate possessing phenolic hydroxyl (Ph) groups, and cellulose nanofiber were extruded to fabricate 3D hydrogel constructs. Lattice- and human nose-shaped 3D constructs were successfully printed and showed good stability in cell culture medium for over a week. Mouse 10T1/2 fibroblasts enclosed in the printed constructs remained viable after 7 days of culture. It was also able to switch a non-cell-adhesive surface of the printed construct to cell-adhesive surface for culturing cells on it through a subsequent cross-linking of gelatin possessing Ph moieties. These results demonstrate the possibility of utilizing the presented cross-linking method for 3D bioprinting.

Keywords: Enzymatic hydrogelation, Horseradish peroxidase, Glucose, Alginate, Cellulose nanofiber, Bioink, Extrusion-based bioprinting

***Corresponding Author:** Shinji Sakai, Department of Materials Engineering Science, Graduate School of Engineering Science, Osaka University, Toyonaka, Osaka 560-8531, Japan; sakai@cheng.es.osaka-u.ac.jp

Received: November 18, 2019; ***Accepted:*** January 02, 2020; ***Published Online:*** January 21, 2020

Citation: Gantumur E, Nakahata M, Kojima M, *et al*., 2020, Extrusion-based bioprinting through glucose-mediated enzymatic hydrogelation. *Int J Bioprint*, 6(1):250. DOI: 10.18063/ijb.v6i1.250.

1 Introduction

Fabrication of three-dimensional (3D) tissues has been a subject of interest in the fields of tissue engineering and regenerative medicine for over the past decades. The classic biofabrication techniques, such as solid or soft material-based scaffolding[1-3] and self-assembling of cell sheets or spheroids[4], have limitations to mimic the structure and function of the natural tissues that are well-organized with multicellular population, a variety of extracellular matrix, growth factors, and bioactive compounds[5]. Recent trend in the fields is 3D bioprinting,[6-8] which enables the deposition of living cells with biomaterials (i.e., bioinks) at micrometer precision to replicate the microarchitecture of targeted tissue[9-11]. Besides, the available bioprinting strategies[12] including inkjet-based[13,14], laser-assisted[15,16], and stereolithography-based[17,18], extrusion-based bioprinting[19] is the most extensively adopted strategy due to its simplicity, printing precision, and a variety of applicable biomaterials. In extrusion bioprinting, viscous solutions are extruded from a nozzle as inks on a substrate surface based on the digital design. The extruded inks must be stabilized into solid hydrogels before spreading for getting the constructs with designed shapes. In general, the stabilization is accomplished through the cross-linking of polymers in the inks resulting in hydrogelation. Various cross-linking methods have been applied to the extrusion bioprinting[20,21].

To fabricate a structure having a complicated structure like natural tissues, we believe that it

is desirable to use multiple materials that give a function suitable for each part and multiple cross-linking systems suitable for each material. Many attempts have been made to develop cross-linking methods which can exert powerful influences on printability, mechanical properties, and cell compatibility of hydrogels. Even today, it is desired to develop a novel bioprinting system that can be achieved by a biocompatible cross-linking process without using toxic substances because it will further enlarge the potential of bioprinting in the fields of tissue engineering and regenerative medicine. The existing cross-linking pathways in bioprinting include physical and chemical cross-linking that rely on external stimuli, such as temperature, ions, or light[22,23]. More recently, enzymatic reactions have newly attracted attention as mild and cell-friendly cross-linking methods for 3D bioprinting[24]. Specifically, bioinks containing horseradish peroxidase (HRP) that has a function to catalyze the conjugation of phenol and aniline derivatives by consuming hydrogen peroxide (H_2O_2) have been used for printing cell-laden microparticles[25], 3D hydrogel constructs[26-28], or patterned hydrogels for cell immobilization[29] using inkjet or extrusion-based bioprinting. Despite the advantage of a wide range of material choices, a major consideration in this reaction system is a way of supplying H_2O_2. To print a 3D hydrogel construct with living cells, the exposure time or the concentration of H_2O_2 should be at non-cytotoxic level and harmless to the activity of the enzyme itself[30]. In the previous studies, H_2O_2 was mixed into an aqueous bath solution[25,26], a hydrogel substrate[29], or another ink[27] to achieve the rapid hydrogelation when it was contacted with the ink containing HRP. Furthermore, there was an approach that uses air containing H_2O_2 instead of an aqueous H_2O_2 solution to control its concentration at the ppm level[28]. All of these approaches are the direct supply of H_2O_2, which might cause inhomogeneity of the resultant hydrogel network as well[31].

Recently, we have developed a way to supply H_2O_2 indirectly to this enzymatic reaction in the presence of reducing sugars, such as glucose, galactose, and mannose[32,33]. In this system, the redox reactions between thiol groups in HRP and formed disulfide bond gradually generate H_2O_2 by consuming reducing sugar under aerobic conditions. It was confirmed that living cells can be enclosed/cultured inside or on the surface of resultant hydrogel with high cell viability and proliferation. Herein, we utilized glucose-mediated enzymatic reaction for extrusion-based bioprinting as a comixable cross-linker with living cells to expand its potential application. Our bioink contains living cells, HRP, a supporting material, polymer possessing phenolic hydroxyl (Ph) groups (Polymer-Ph), and reducing sugar (**Figure 1**). Alginate and glucose were chosen as a representative polymer chain and reducing sugar. In a preliminary study of the application of the cross-linking system, we realized that a drawback of the system was a non-instantaneous hydrogelation of deposited ink. A possible approach to suppress a dispersion of the deposited ink was an enhancement of the viscosity of ink. To enhance the viscosity of ink and the shape fidelity of printed constructs until the stabilization through the enzyme-mediated

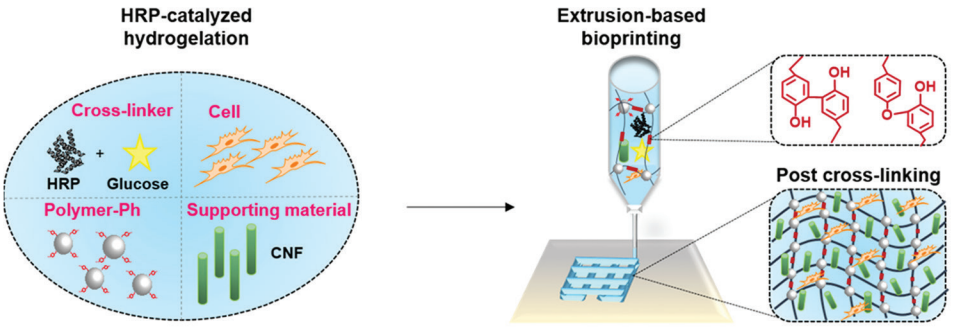

Figure 1. Schematic of extrusion-based bioprinting through glucose-mediated enzymatic hydrogelation.

cross-linking, a dispersion of cellulose nanofibers (CNF) was incorporated as a supporting material. CNF has already made an impact in the field of bioprinting due to its outstanding shear thinning and mechanical properties[34]. The combination of alginate and CNF has been previously used for bioink and separately treated with calcium ions for postcross-linking[35-37]. In this study, the cross-linker (i.e., enzyme and glucose) mixed in the bioink led to a slow hydrogelation during and the following printing step while CNF supported well the stability of complex construct. In addition to the printability, the cell behavior inside or on the surface of gelatin-coated hydrogel was investigated to ensure the cell compatibility of the proposed method.

2 Materials and methods

2.1 Materials

Sodium alginate (Kimica I-1G, high content of guluronic acid and molecular weight, 70 kDa), gelatin (type B from bovine skin), and CNF suspension (Rheocrysta I-2SX, dry CNF content, 2 w/v%) were purchased from Kimica (Tokyo, Japan), Kewpie (Tokyo, Japan), and DKS Co. Ltd. (Kyoto, Japan). HRP (200 units/mg), D-glucose, and *N*-hydroxysulfosuccinimide (NHS) were obtained from FUJIFILM Wako Pure Chemical Corporation (Osaka, Japan). Water-soluble carbodiimide (WSCD) and tyramine hydrochloride were purchased from Peptide Institute (Osaka, Japan) and Chem-Impex International (Wood Dale, IL, USA), respectively. 3-(4-hydroxyphenyl) propionic acid and rhodamine (Rho) were purchased from Tokyo Chemical Industry (Tokyo, Japan). Alginate (Alg-Ph, 1.4×10^{-4} mol-Ph/g) and gelatin (Rho-Gel-Ph, 1.5×10^{-4} mol-Ph/g) derivatives possessing Ph groups were synthesized by conjugating tyramine hydrochloride using NHS and WSCD, as previously reported[38,39]. Mouse 10T1/2 fibroblast cells were provided by Riken Cell Bank (Ibaraki, Japan) and cultured in Dulbecco's Modified Eagle's Medium (DMEM, Nissui, Tokyo, Japan) supplemented with 10% fetal bovine serum at 37°C in 5% CO_2.

2.2 Ink preparation and rheological characterization

Phosphate-buffered saline (PBS, pH 7.4) containing Alg-Ph (0.5 w/v%), HRP (100 units/mL), and D-glucose (44 mg/mL) was prepared. As a supporting material, CNF (autoclaved at 121°C for 20 min, 0.5~1.5 w/v%) was added. The rheological properties of the prepared bioinks were analyzed using a rheometer (HAAKE MARS III, Thermo Fisher Scientific, MA, USA) with a parallel plate of 20 mm radius at 25°C, immediately after mixing. Dynamic viscoelasticity measurement was performed at a constant shear strain of 1% and the gap between the parallel plate and the stage was set to 1 mm.

2.3 Bioprinting procedure

The prepared inks were printed using a software-assisted 3D printer (Reprap Prusa i3, HIC Technology Co. Ltd., Hong Kong, China) modified to have one syringe connected to a syringe pump. The inks were extruded from a 27-gauge stainless needle at 22 mm/s onto the stage moving at 22 mm/s to build lattice- (20×21 mm^2, thickness 1 mm, 10 layers) and a human nose-shaped (12×15 mm^2, thickness 7 mm, 70 layers at maximum) 3D hydrogel constructs. The thickness of a layer was set at 0.1 mm. The bioprinting process was carried out at room temperature and the obtained constructs were rested at room temperature for 2 h after printing to let the postcross-linking.

2.4 Swelling of hydrogel in medium

PBS containing Alg-Ph (0.5 w/v%), HRP (100 units/mL), D-glucose (44 mg/mL), and CNF (1.5 w/v%) was poured into PDMS mold and rested at room temperature for 2 h to obtain disk-shaped hydrogel with 15 mm in diameter. The resultant hydrogels were then soaked in DMEM. The medium was changed every day. The diameter of the specimen was measured using the software Image J (National Institutes of Health, USA).

2.5 Cell behavior in hydrogel

10T1/2 cells were suspended in PBS containing Alg-Ph (0.5 w/v%), HRP (100 units/mL),

D-glucose (44 mg/mL), and CNF (1.5 w/v%) at 5 × 10^5 cells/mL, as a bioink. The cell-laden lattice-shaped constructs were printed in a safety cabinet and kept in an incubator until the complete cross-linking. As a non-printed hydrogel, the mixture solution was poured into 24-well plate at 0.25 mL/well. The resultant hydrogels were incubated in DMEM at 37°C. After 1 day and 7 days of incubation, the cells in hydrogels were stained with Calcein-AM (live cells) and propidium iodide (dead cells) for the observation using a fluorescence microscope (BZ-9000, Keyence Corp., Osaka, Japan).

2.6 Switching hydrogel surface

Lattice-shaped hydrogel construct was printed first using the selected ink on a culture dish with a surface covered with 1.0% agarose gel. After post-cross-linking, the hydrogel construct was soaked in a solution containing Rho-Gel-Ph (1.0 w/v%) for overnight at 37°C. Then, the construct was rinsed well with PBS to remove

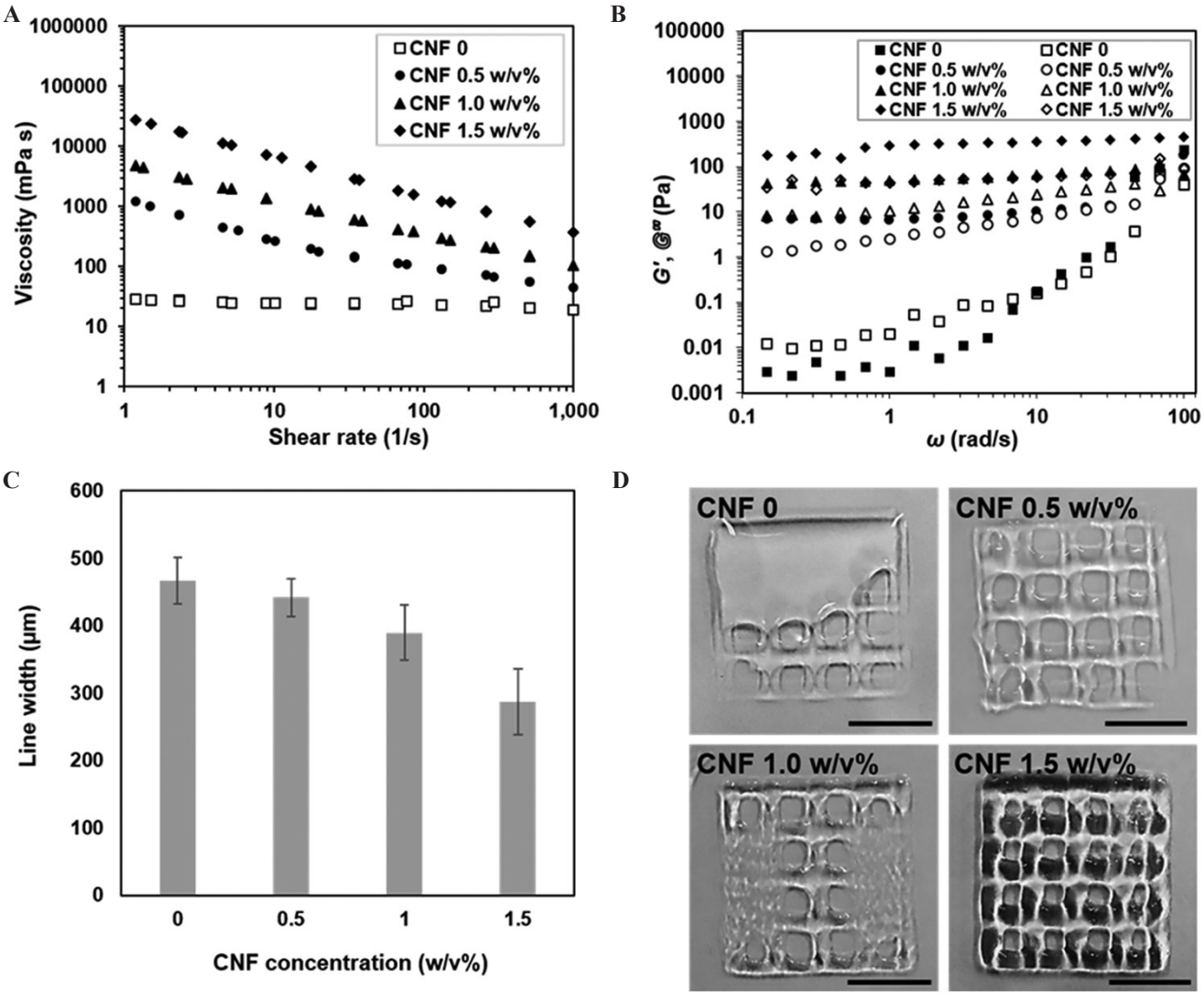

Figure 2. Rheological properties and printability of inks containing different concentrations of CNF: (A) Viscosity changes at various shear rates. (B) Storage modulus, G' (closed symbols) and loss modulus, G'' (open symbols) as a function of angular frequency. (C) Width measurement of the printed lines. Data are mean ± SD (n = 6). (D) Printed lattice-shaped constructs. Scale bars: 1 cm.

the non-cross-linked Rho-Gel-Ph. Subsequently, 10T1/2 cells were seeded at 1×10^4 cells/cm^2 and incubated in DMEM at 37°C.

3 Results and discussion

3.1 Characterization and printability of inks

To determine the optimal printing condition of CNF and alginate-based ink, the variable concentrations of CNF (from 0 to 1.5 w/v%) and the fixed concentration of Alg-Ph (0.5 w/v%) were mixed to prepare four different inks. The concentrations of HRP (100 units/mL) and glucose (44 mg/mL) were determined based on the previous findings in terms of gelation time[32,33]. Comparing to the direct supply of H_2O_2 as an aqueous solution[38], the gelation time of this method is much longer and that makes it possible to mix all the ink components at the same time. **Figure 2A** shows the viscosity changes of the prepared inks at various shear rates. The ink non-containing CNF (CNF 0) has low zero-shear viscosity at the beginning of cross-linking resulting in a poor shape fidelity during the printing (**Figure 2D**). The viscosity of Alg-Ph solution gradually increased with increasing the concentration of incorporated CNF. As already known[35], the shear-thinning property of the ink containing CNF was confirmed by showing high viscosity at low shear rates and low viscosity at high shear rates. Dynamic viscoelastic measurements in **Figure 2B** also show that the storage modulus (G') and loss modulus (G'') substantially increased with a higher proportion of CNF in the ink. These rheological responses of the prepared inks were in agreement with the printing resolution indicated by the widths of printed lines (**Figure 2C**). The inks with higher viscosities improved the printing resolution. Then, the high printing resolution gave nicely printed lattice-shaped hydrogel construct (**Figure 2D**). Based on the results, the ink containing 1.5 w/v% CNF was selected from the prepared inks as an appropriate ink for printing. Incorporating more high concentration of CNF into the ink caused nozzle clogging.

Once an optimal concentration of CNF incorporated in the ink was determined, a more complex construct was printed. It was previously noted that CNF can mimic the bulk collagen matrix for cartilage tissue[40]. Thus, the hydrogel construct resembling human nose, which is one of the cartilage tissues was successfully printed using the selected ink. Even during up to 20 min of printing procedure and slow cross-linking process, the printed construct maintained its shape without collapsing (**Figure 3A**). In addition, if it is required to let the cross-linking more slowly for longer printing procedure, the concentrations of HRP and glucose can be decreased[32,33]. After cross-linked through glucose-mediated HRP-catalyzed reaction, the printed human nose construct became mechanically stable and showed elastic deformation after squeezing (**Figure 3B**).

Furthermore, the stability of hydrogel after cross-linking in cell culture medium was examined before evaluating the cell behavior inside it. The diameters of disk-shaped hydrogels obtained using the selected ink increased <15% when compared with their initial sizes for the first 2 days of soaking in medium. After that, the changes in the size of hydrogels were barely noticeable and stayed stable during the 8 days of soaking (**Figure 4**). Taken together the results from rheology, printability, and stability, it is possible to print complex and stable hydrogel constructs with good shape fidelity using the proposed ink and the cross-linking method.

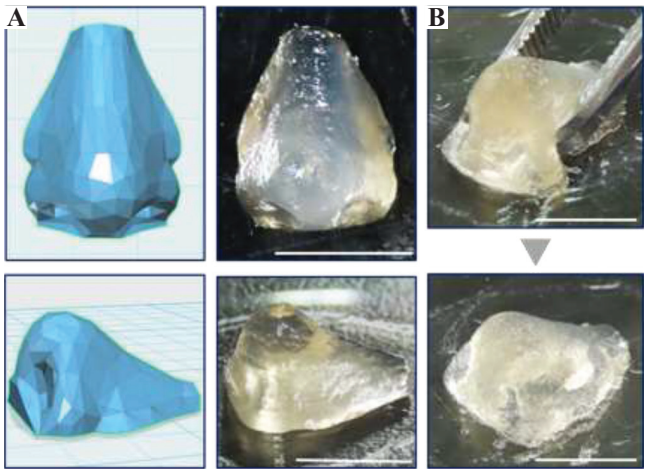

Figure 3. Printed human nose construct based on blueprint (A) before and (C) after postcross-linking. Scale bars: 1 cm.

3.2 Cell behavior in the printed construct

To ensure the feasibility of applying the proposed bioink and cross-linking method for printing living cells, the cell-laden lattice-shaped constructs were prepared. Mouse 10T1/2 fibroblasts were chosen as a model cell line for the cell studies. As non-printed hydrogels for comparison, the hydrogels were prepared in cell culture well plate using the same bioink. As shown in **Figure 5**, the homogeneous distributions of viable cells were observed in both non-printed (50.1 ± 0.4% viability, n=3) and printed hydrogels (54.1 ± 0.6% viability, n=3) after 1 day of culture. These similar cell viabilities indicate that there were no harmful effects on the cells by printing with the proposed cross-linking method. Moreover, the printed construct stably maintained its shape and dimension even after 7 days of culture in the presence of cells. The cell viability in the construct (56.0 ± 2.4%, n = 3) at day 7 was found to be higher than that in the non-printed hydrogel (44.3 ± 2.5%, n=3). The reason of this difference in cell viability may be due to the different internal architecture of the printed and non-printed bulk hydrogel. It was reported that the internal geometrical features of cell enclosed hydrogel have influence on cell fate[41]. However, the decreases of cell density in both hydrogels were observed. This is most likely attributed to the dead cells that were not stained due to the cell

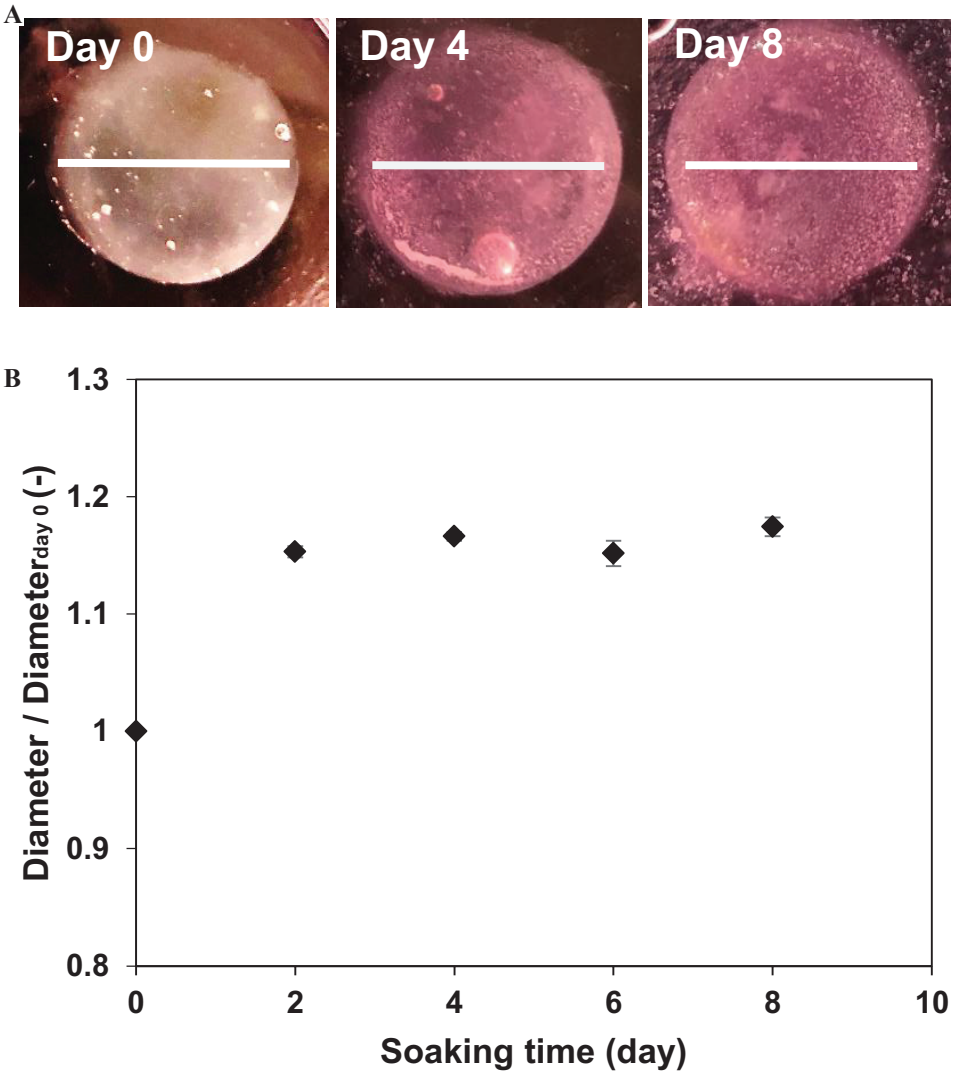

Figure 4. (A) Photographs of disk-shaped hydrogels after soaking in cell culture medium for 0, 4, and 8 days. Scale bars: 1.5 cm. (B) Change in diameter of hydrogels. Data are mean ± SD (n = 3).

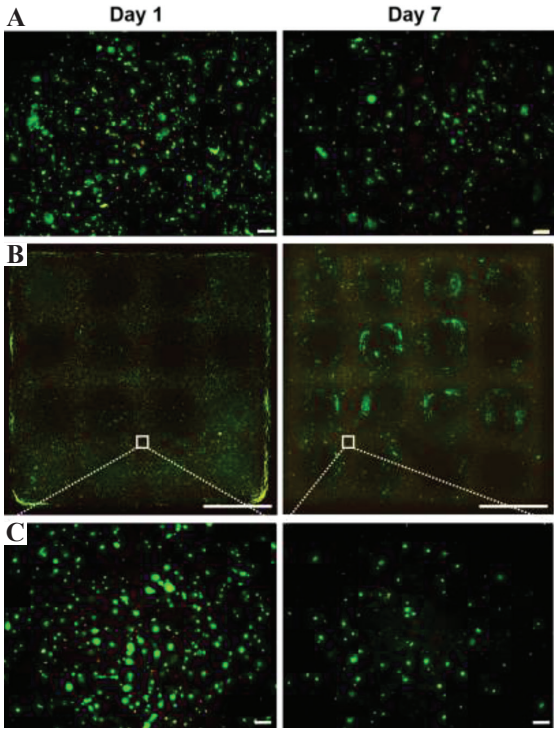

Figure 5. Fluorescence images of 10T1/2 cells cultured in (A) non-printed and (B, C) printed hydrogels for 1 and 7 days at different magnifications. Live and dead cells show green and red fluorescence, respectively. Scale bars: (A), (C) 200 μm and (B) 5 mm.

lysis. The possible reason for cell death might be the mechanical stress from the high concentration of CNF incorporated in the hydrogels during the mixing procedure and the culture time. In the previous study that also used CNF for the extrusion system, low cell viability (<70%) for human chondrocytes, which has different morphology than our model cell line, was reported. It could be considered as one of the drawbacks of using CNF for bioink[35]. Although it is out of the scope of this paper, CNF-based bioinks may be more suitable for the regeneration of cartilage tissues than the other tissues[40,42]. Besides this effect of CNF on cells, the proposed hydrogelation method can be utilized for 3D bioprinting of living cells.

3.3 Switchable construct surface

3D-printed hydrogel constructs can also be used as scaffolds for cell culture[43,44]. Since it is well-known that alginate has no binding site for cell adhesion[45], we made an attempt to switch the surface of a printed construct for cell culture. Taking advantage of the possibility to cross-link various polymers through the same enzymatic reaction, Gel-Ph was selected as a coating

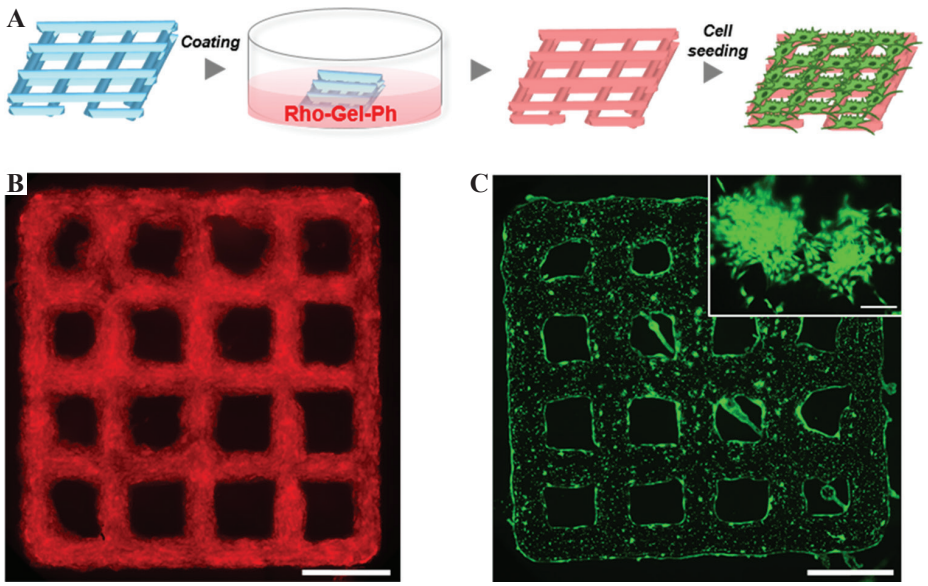

Figure 6. (A) Workflow of switching hydrogel surface after printing and postcross-linking. Fluorescence images of (B) printed lattice-shaped hydrogel after coating and (C) 10T1/2 cells cultured on the hydrogel for 2 days. The image (scale bar: 200 μm) in upper right corner shows the sign of cell elongation. Scale bars: (B) and (C) 5 mm.

material due to its ability to promote cell adhesion and proliferation. The lattice-shaped construct obtained using the selected ink was soaked in a solution containing rhodamine-labeled Gel-Ph (1.0 w/v%, Rho-Gel-Ph) right after printing (**Figure 6A**). Due to the remaining HRP and glucose, Gel-Ph can be cross-linked with non-cross-linked Ph moieties in the hydrogel. After 1 day of soaking, the entire surface of the lattice-shaped construct had a strong signal of red fluorescence derived from Rho-Gel-Ph, which indicates the successful coating process (**Figure 6B**). Subsequently, 10T1/2 cells were seeded on the construct to confirm the switched culture surface. As shown in **Figure 6C**, the cells adhered to and elongated on the entire surface of the construct. These results demonstrate that it is possible to switch non-cell-adhesive surface of the printed construct to cell-adhesive surface with a simple procedure. Moreover, the ability to modify the surface with desired materials through the proposed method enables to design functionalized 3D construct for individual applications.

4 Conclusions

We demonstrated the feasibility of utilizing glucose-mediated enzymatic hydrogelation for extrusion-based bioprinting. The cross-linking of Alg-Ph and CNF-based bioink through HRP-catalyzed reaction that consumes H_2O_2 generated by HRP and glucose enabled to print 3D cell-laden construct with good shape fidelity. The cell-laden construct was successfully cultured for 7 days without collapsing. In addition to the potency of printing with living cells, it was also demonstrated that the printed construct can be used as a scaffold for cell culture after coated with Gel-Ph through the same cross-linking method. Overall, the proposed method advances the ability of bioprinting with living cells with a mild and cell compatible cross-linking.

Acknowledgments

This work was supported by the Japan Society for the Promotion of Science (JSPS) KAKENHI Grant Numbers 15H04194, 16H02423, 17H03472, 18H01797 and Grand-In-Aid for JSPS Fellows 18J11601.

Conflicts of interest

There are no conflicts of interest to declare.

References

1. An J, Teoh JEM, Suntornnond R, *et al.*, 2015, Design and 3D Printing of Scaffolds and Tissues. *Engineering*, 1(2):261–8. DOI 10.15302/J-ENG-2015061.
2. Liu F, Mishbak H, Bartolo P, *et al.*, 2019, Hybrid Polycaprolactone/Hydrogel Scaffold Fabrication and In-process Plasma Treatment Using PABS. *Int J Bioprint*, 5(1):174. DOI: 10.18063/ijb.v5i1.174.
3. Yang Y, Wang G, Liang H, *et al.*, 2019, Additive Manufacturing of Bone Scaffolds. *Int J Bioprint*, 5(1):148. DOI: 10.18063/ijb.v5i1.148.
4. Zhuang P, Sun AX, An J, *et al.*, 2018, 3D Neural Tissue Models: From Spheroids to Bioprinting. *Biomaterials*, 154:113–33. DOI: 10.1016/j.biomaterials.2017.10.002.
5. Mironov V, Trusk T, Kasyanov V, *et al.*, 2009, Biofabrication: A 21st Century Manufacturing Paradigm. *Biofabrication*, 1(2):022001. DOI: 10.1088/1758-5082/1/2/022001.
6. Mir TA, Nakamura M, Iwanaga S, *et al.*, 2019, Biofabrication Offers Future Hope for Tackling Various Obstacles and Challenges in Tissue Engineering and Regenerative Medicine: A Perspective, *Int J Bioprint*, 5(1):153. DOI: 10.18063/ijb.v5i1.153.
7. Ng WL, Chua CK, Shen YF, *et al.*, 2019, Print Me an Organ! Why We are not There Yet. *Prog Polym Sci*, 97:101145. DOI: 10.1016/j.prog-polymsci.2019.101145.
8. Lee JM, Sing SL, Zhou M, *et al.*, 2018, 3D Bioprinting Processes: A Perspective on Classification and Terminology. *Int J Bioprint*, 4(2):151. DOI: 10.18063/ijb.v4i2.151.
9. Murphy SV, Atala A, 2014, 3D Bioprinting of Tissues and Organs. *Nat Biotechnol*, 32(8):773–85. DOI: 10.1038/nbt.2958.
10. Du X, 2018, 3D Bio-Printing Review. *Mater Sci Eng*, 301(1):012023. DOI: 10.1088/1757-899X/301/1/012023.
11. Heinrich MA, Liu W, Jimenez A, *et al.*, 2019, 3D Bioprinting: From Benches to Translational Applications. *Small*, 15(23):1805510. DOI: 10.1002/smll.201805510.
12. Lee JY, An J, Chua CK, *et al.*, 2017, Fundamentals and Applications of 3D Printing for Novel Materials. *Appl Mater Today*, 7:120–33. DOI: 10.1016/j.apmt.2017.02.004.
13. Nakamura K, Nishiyama Y, Henmi C, *et al.*, 2008, Ink

Jet Three-dimensional Digital Fabrication for Biological Tissue Manufacturing: Analysis of Alginate Microgel Beads Produced by Ink Jet Droplets for Three Dimensional Tissue Fabrication. *J Imaging Sci Technol*, 52(6):060201. DOI: 10.2352/J.ImagingSci.Technol.(2008)52:6(060201).

14. Arai K, Iwanaga S, Toda H, *et al.*, 2011, Three-Dimensional Inkjet Biofabrication Based on Designed Images. *Biofabrication*, 3(3):034113. DOI: 10.1088/1758-5082/3/3/034113.
15. Sorkio A, Koch L, Koivusalo L, *et al.*, 2018, Human Stem Cell Based Corneal Tissue Mimicking Structures Using Laser-Assisted 3D Bioprinting and Functional Bioinks. *Biomaterials*, 171:57–71. DOI: 10.1016/j.biomaterials.2018.04.034.
16. Kérourédan O, Hakobyan D, Rémy M, *et al.*, 2019, *In Situ* Prevascularization Designed by Laser-assisted Bioprinting: Effect on Bone Regeneration. *Biofabrication*, 11(4):045002. DOI: 10.1088/1758-5090/ab2620.
17. Sakai S, Kamei H, Mori T, *et al.*, 2018, Visible Light-Induced Hydrogelaton of an Alginate Derivative and Application to Stereolithographic Bioprinting Using a Visible Light Projector and Acic Red. *Biomacromolecules,* 19(2):672–9. DOI: 10.1021/acs.biomac.7b01827.
18. Lam T, Dehne T, Krüger JP, *et al.*, 2019, Photopolymerizable Gelatin and Hyaluronic Acid for Stereolithographic 3D Bioprinting of Tissue-Engineered Cartilage. *J Biomed Mater Res B,* 107(8):2649–57. DOI: 10.1002/jbm.b.34354.
19. Zhuang P, Ng WL, An J, *et al.*, 2019, Layer-By-Layer Ultraviolet Assisted Extrusion-Based (UAE) Bioprinting of Hydrogel Constructs with High Aspect Ratio for Soft Tissue Engineering Applications. *Plos One*, 14(6):e0216776. DOI: 10.1371/journal.pone.0216776.
20. Placone JK, Engler AJ, 2018, Recent Advances in Extrusion-Based 3D Printing for Biomedical Applications. *Adv Healthc Mater,* 7(8):e1701161. DOI: 10.1002/adhm.201701161.
21. Tai C, Bouissil S, Gantumur E, *et al.*, 2019, Use of Anionic Polysaccharides in the Development of 3D Bioprinting Technology. *Appl Sci,* 9(13):2596. DOI: 10.3390/app9132596.
22. Hölzl K, Lin S, Tytgat L, *et al.*, 2016, Bioink Properties Before, During and After 3D Bioprinting. *Biofabrication*, 8(3):032002. DOI: 10.1088/1758-5090/8/3/032002.
23. Ji S, Guvendiren M, *et al.*, 2017, Recent Advances in Bioink Design for 3D Bioprinting of Tissues and Organs. *Front Bioeng Biotechnol*, 5:23. DOI: 10.3389/fbioe.2017.00023.
24. Das S, Pati F, Choi YJ, *et al.*, 2015, Bioprintable, Cell-Laden Silk Fibroin-Gelatin Hydrogel Supporting Multilineage Differentiation of Stem Cells for Fabrication of Three-Dimensional Tissue Constructs. *Acta Biomater*, 11:233–46. DOI: 10.1016/j.actbio.2014.09.023.
25. Sakai S, Yamamoto Y, Enkhtuul G, *et al.*, 2017, Inkjetting Plus Peroxidase-Mediated Hydrogelation Produces Cell-laden, Cell-Sized Particles with Suitable Characters for Individual Applications. *Macromol Biosci*, 17(5):1600416. DOI: 10.1002/mabi.201600416.
26. Arai K, Tsukamoto Y, Yoshida H, *et al.*, 2016, The Development for Cell-Adhesive Hydrogel for 3D Printing. *Int J Bioprinting*, 2(2):44–53. DOI: 10.18063/IJB.2016.02.002.
27. Sakai S, Ueda K, Gantumur E, *et al.*, 2018, Drop-on-Drop Multimaterial 3D Bioprinting Realized by Peroxidase-Mediated Cross-Linking. *Macromol Rapid Commun*, 39(3):1700534. DOI: 10.1002/marc.201700534.
28. Sakai S, Mochizuki K, Qu Y, *et al.*, 2018, Peroxidase-Catalyzed Microextrusion Bioprinting of Cell-Laden Hydrogel Constructs in Vaporized Ppm-Level Hydrogen Peroxide. *Biofabrication*, 10(4):045007. DOI: 10.1088/1758-5090/aadc9e.
29. Gantumur E, Kimura M, Taya M, *et al.*, 2020, Inkjet Micropatterning Through Horseradish Peroxidase-mediated Hydrogelation for Controlled Cell Immobilization and Microtissue Fabrication. *Biofabrication*, 12(1):011001. DOI: 10.1088/1758-5090/ab3b3c.
30. Sakai S, Nakahata M, *et al.*, 2017, Horseradish Peroxidase Catalyzed Hydrogelation for Biomedical, Biopharmaceutical, and Biofabrication Applications. *Chem Asian J*, 12(24):3098–109. DOI: 10.1002/asia.201701364.
31. Moriyama K, Minamihata K, Wakabayashi R, *et al.*, 2014, Enzymatic Preparation of a Redox-Responsive Hydrogel for Encapsulating and Releasing Living Cells. *Chem Commun*, 50(44):5895–8. DOI: 10.1039/c3cc49766f.
32. Gantumur E, Sakai S, Nakahata M, *et al.*, 2017, Cytocompatible Enzymatic Hydrogelation Mediated by Glucose and Cysteine Residues. *ACS Macro Lett*, 6(5):485–8. DOI: 10.1021/acsmacrolett.7b00122.
33. Gantumur E, Sakai S, Nakahata M, *et al.*, 2019, Horseradish Peroxidase-Catalyzed Hydrogelation Consuming Enzyme-Produced Hydrogen Peroxide in the Presence of Reducing Sugars. *Soft Matter*, 15(10):2163–9. DOI: 10.1039/c8sm01839a.
34. Athukoralalage SS, Balu R, Dutta NK, *et al.*, 2019, 3D Bioprinted Nanocellulose-Based Hydrogels for Tissue Engineering Applications: A Brief Review. *Polymers*, 11(5):898. DOI: 10.3390/polym11050898.
35. Markstedt K, Mantas A, Tournier I, *et al.*, 2015, 3D Bioprinting Human Chondrocytes with Nanocellulose-Alginate Bioink for Cartilage Tissue Engineering Application. *Biomacromol*,

16(5):1489–96. DOI: 10.1021/acs.biomac.5b00188.

36. Leppiniemi J, Lahtinen P, Paajanen A, *et al.*, 2017, 3D-Printable Bioactivated Nanocellulose-Alginate Hydrogels. *ACS Appl Mater Interfaces*, 9(26):21959–70. DOI: 10.1021/acs.ami.7b02756.
37. Ojansivu M, Rashad A, Ahlinder A, *et al.*, 2019, Wood-Based Nanocellulose and Bioactive Glass Modified Gelatin-Alginate Bioinks for 3D Bioprinting of Bone Cells. *Biofabrication*, 11(3):035010. DOI: 10.1088/1758-5090/ab0692.
38. Sakai S, Kawakami K, *et al.*, 2007, Synthesis and Characterization of Both Ionically and Enzymatically Cross-linkable Alginate. *Acta Biomater*, 3(4):495–501. DOI: 10.1016/j.actbio.2006.12.002.
39. Sakai S, Hirose K, Taguchi K, *et al.*, 2009, An Injectable, In Situ Enzymatically Gellable, Gelatin Derivative for Drug Delivery and Tissue Engineering. *Biomaterials*, 30(20):3371-7. DOI: 10.1016/j.biomaterials.2009.03.030.
40. Nguyen D, Hägg DA, Forsman A, *et al.*, 2017, Cartilage Tissue Engineering by the 3D Bioprinting of iPS Cells in a Nanocellulose/Alginate Bioink. *Sci Reports*, 7(1):658. DOI: 10.1038/s41598-017-00690-y.
41. Wang L, Xu M, Luo L, *et al.*, 2018, Iterative Feedback Bio-printing-derived Cell-laden Hydrogel Scaffolds with Optimal Geometrical Fidelity and Cellular Controllability. *Sci Rep*, 8(1):2802. DOI: 10.1038/s41598-018-21274-4.
42. Piras CC, Fernandez-Prieto S, De Borggraeve WM, *et al.*, 2017, Nanocellulosic Materials as Bioinks for 3D Bioprinting. *Biomater Sci*, 5(10):1988–92. DOI: 10.1039/c7bm00510e.
43. Xu W, Zhang X, Yang P, *et al.*, 2019, Surface Engineered Biomimetic Inks Based on UV Cross-Linkable Wood Biopolymers for 3D Printing. *Appl Mater Interfaces*, 11(13):12389–400. DOI: 10.1021/acsami.9b03442.
44. Ajdary R, Huan S, Ezazi NZ, *et al.*, 2019, Acetylated Nanocellulose for Single-Component Bioinks and Cell Proliferation on 3D-Printed Scaffolds. *Biomacromol*, 20(7):2770–8. DOI: 10.1021/acs.biomac.9b00527.
45. Sarker B, Singh R, Silva R, *et al.*, 2014, Evaluation of Fibroblasts Adhesion and Proliferation on Alginate-Gelatin Crosslinked Hydrogel. *Plos One*, 9(9):e107952. DOI: 10.1371/journal.pone.0107952.